

## **Supplementary Material**

**for**

### **Effects of nitrate and nitrite on UV/PDS process: performance and byproducts formation from the aspect of substituent**

Yawei Xie<sup>1</sup>, Chenda Wu<sup>1</sup>, Yue Wang<sup>1</sup>, Shijie Wu<sup>1</sup>, Yaozu Jin<sup>1</sup>, Mingdi Yang<sup>1</sup>, Hongyuan Liu<sup>1\*</sup>

<sup>1</sup> College of Civil Engineering, Zhejiang Key Laboratory of Civil Engineering Structures & Disaster Prevention and Mitigation Technology, Zhejiang University of Technology, Hangzhou, 310023, China

\*Corresponding author

Hongyuan Liu, E-mail: lhyzyy@zjut.edu.cn

## List of Supplementary materials

Text S1 Chemicals and reagents

Text S2 Calculation of reaction stoichiometric efficiency

Text S3 Determination of the contribution of each free radical

Text S4 Detection methods

Text S5 Methods for Fourier transform ion cyclotron resonance mass spectrometer (FT-ICR-MS) and data analysis

Fig. S1 kinetic of pollutants' removal

Fig. S2 kinetic of pollutants' removal in UV/PDS with different addition of  $\text{NO}_3^-$

Fig. S3 a Absorbance of  $\text{NO}_3^-$ ,  $\text{NO}_2^-$  and the three compounds, b Absorbance of three compounds with the addition of  $\text{NO}_3^-/\text{NO}_2^-$

Fig. S4 pH variation during the reaction

Fig. S5 The HOMO and LUMO distribution of Ph, BA and SA calculated at B3LYP/6-31+G(d) level.

Fig. S6 FT IR spectra of three compounds before and after treatment with species

Fig. S7 Van Krevelen diagrams of potentially formed CHO (blue) and CHNO (red) of Ph, BA and SA during UV/PDS oxidation in the presence of  $\text{NO}_3^-$  and  $\text{NO}_2^-$

Fig. S8 Molecule number of byproducts of Ph, BA and SA treated by UV/PDS in the presence of  $\text{NO}_3^-$  and  $\text{NO}_2^-$

Fig. S9 Distribution of molecule mass of byproducts of Ph, BA and SA in UV/PDS in the presence of  $\text{NO}_3^-$  and  $\text{NO}_2^-$

Table S1 Comparison of the reaction stoichiometric efficiency in different systems

Table S2 Calculated condensed Fukui function and dual descriptor of Ph

Table S3 Calculated condensed Fukui function and dual descriptor of BA

Table S4 Calculated condensed Fukui function and dual descriptor of SA

### Text S1 Chemicals and reagents

Sodium persulfate ( $\text{Na}_2\text{S}_2\text{O}_8$ ) was purchased from Shanghai Aladdin Biochemical Technology Co., Ltd.; Sodium nitrate ( $\text{NaNO}_3$ , 99%), sodium thiosulfate ( $\text{Na}_2\text{S}_2\text{O}_3$ ) were purchased from Shanghai Lingfeng Chemical Reagent Co., Ltd.; Sodium nitrite ( $\text{NaNO}_2$ ), phenol, phosphoric acid ( $\text{H}_3\text{PO}_4$ ), were purchased from Sinopharm Chemical Reagent Co., Ltd.; Benzoic acid and salicylic acid were purchased from Hangzhou Jigong Biotechnology Co., Ltd.; High-performance liquid chromatography (HPLC)-grade methanol, acetonitrile were purchased from Shanghai Titan Technology Co., Ltd.

### Text S2 Calculation of reaction stoichiometric efficiency

The reaction stoichiometric efficiency (%RSE) means the number of moles of the organic contaminants degraded versus the number of mole of PS consumed. The organic contaminants is detection by HPLC refer to the later sections. Persulfate anion concentration was determined on a TU-1901 UV-VIS spectrophotometer. The analysis of absorption spectra of a yellow colored solution resulting from the reaction of PS and iodide in the presence of sodium bicarbonate reveals an absorbance at 352 nm, without significant interferences from the reagent matrix. 0.5 mL were withdrawn from the reactor each 10 min and added into a 10 mL vial containing 4.0 mL of 10 g/L KI solution and 0.5 mL of  $\text{NaHCO}_3$  solution. The solution was then mixed and kept in dark for 30 min for the complexation reaction to be completed. PS calibration curves were performed within a range of concentrations of 100-500  $\mu\text{M}$ .

### Text S3. Determination of the contribution of each free radical

The *tert*-butanol (TBA) was added into the UV/peroxydisulfate (PDS) process to create a scenario of  $\text{SO}_4^{\cdot-}$ . Because  $\text{HO}^{\cdot}$  was completely consumed by TBA because nitrobenzene was not degraded by UV/PDS/TBA. Therefore, the second-order rate constants of the 3 compounds reacting with  $\text{SO}_4^{\cdot-}$  can be calculated from eq. S2.

$$\ln \left( \frac{[\text{C}]_0}{[\text{C}]_t} \right) / \ln \left( \frac{[\text{BA}]_0}{[\text{BA}]_t} \right) = \frac{k_{\text{T-SO}_4^{\cdot-}}}{k_{\text{BA-SO}_4^{\cdot-}}} \quad (\text{S1})$$

$[\text{C}]_0$  and  $[\text{BA}]_0$  here represent the initial concentrations of the SA and BA, respectively.  $k_{\text{SO}_4^{\cdot-}\text{-T}}$  and  $k_{\text{SO}_4^{\cdot-}\text{-BA}}$  represent the second-order rate constants for  $\text{SO}_4^{\cdot-}$  reacting with SA and BA, respectively.

Nitrobenzene (NB) was used as probes to calculate the reaction rate of various radicals<sup>1</sup>. Oxidation of nitrobenzene was carried out and the concentration of  $\cdot\text{OH}$  was obtained using Eq.S2.

$$k_{\text{obs,NB}} = k_{\text{obs,UV-NB}} + k_{\text{obs,Vol-NB}} + k_{\text{OH}\cdot\text{-NB}}[\text{OH}^{\cdot}]_{\text{ss}} \quad (\text{S2})$$

where:  $k_{\text{obs,NB}}$ ,  $k_{\text{obs,UV-NB}}$  ( $0.0010 \text{ min}^{-1}$ ),  $k_{\text{obs,Vol-NB}}$  ( $0.0024 \text{ min}^{-1}$ ) denote the proposed primary kinetic constants for the degradation of NB in the systems of UV/PDS with the absence and presence of  $\text{NO}_3^-/\text{NO}_2^-$ , UV radiation and stirred volatilization, respectively;  $k_{\text{OH}\cdot\text{-NB}}$  denotes the secondary reaction rate constant of NB with  $\cdot\text{OH}$  ( $3.9 \times 10^9 \text{ M}^{-1}\text{s}^{-1}$ )<sup>2</sup>.

The  $[\text{SO}_4^{\cdot-}]_{\text{ss}}$  in UV/PDS/ $\text{NO}_2^-$  can be calculated according to eq. S3. And the  $[\text{SO}_4^{\cdot-}]_{\text{ss}}$  in the UV/PDS/ $\text{NO}_3^-$  can also be calculated by eq. S3 with the addition of TBA, because TBA can also quench  $\cdot\text{OH}$ .

$$k'_{\text{BA}} = k_{\text{BA-SO}_4^{\cdot-}}[\text{SO}_4^{\cdot-}]_{\text{ss}} + k'_{\text{UV-BA}} \quad (\text{S3})$$

$k'_{BA}$  here is the pseudo-first order rate constant ( $k'$ ) of BA degradation by the UV/PDS in the absence or presence of  $\text{NO}_2^-$  or/and  $\text{NO}_3^-$ .  $k'_{\text{UV-BA}}$  is  $k'$  for BA by UV direct photolysis.  $k_{\text{BA-SO}_4^-}$  represent the  $k_s$  of  $\text{SO}_4^{\cdot-}$  reacting with BA,  $1.2 \times 10^9 \text{ M}^{-1} \text{ s}^{-1}$ .

After determining the  $[\text{SO}_4^{\cdot-}]_{ss}$  and  $[\text{OH}^{\cdot}]_{ss}$  of each system, the contribution reaction rate of each free radical was obtained by eq.S4, without considering the rate of stirring volatilization loss.

$$k_{obs,T} = k_{obs,UV-T} + k_{T\cdot OH} [\cdot OH]_{ss} + k_{T\cdot SO_4^{\cdot-}} [\text{SO}_4^{\cdot-}]_{ss} + k_{obs,RNS-T} \quad (\text{S4})$$

where:  $k_{obs,T}$ ,  $k_{obs,UV-T}$  denote the proposed primary kinetic constants for the degradation of Ph/BA/SA in the systems of UV/PDS with the absence and presence of  $\text{NO}_3^-/\text{NO}_2^-$ , UV radiation respectively;  $k_{T\cdot OH}$ ,  $k_{T\cdot SO_4^{\cdot-}}$  denotes the secondary reaction rate constant of Ph/BA/SA with  $\cdot\text{OH}$  and  $\text{SO}_4^{\cdot-}$ ,  $k_{obs,RNS-T}$  denote the proposed primary kinetic constants for RNS.

#### **Text S4. Detection methods**

For the detection of Ph, the mobile phase consisted of methanol and water (75/25, v/v) at a flow rate of 1 mL/min. The detection wavelength is 269 nm.

For the detection of BA and SA, the mobile phase was methanol and 1% phosphoric acid (50:50, v/v) at a flow rate of 1 mL/min. The detection wavelength is 230 nm.

For the detection of NB, the mobile phase was acetonitrile and water (65:35, v/v) at a flow rate of 1 mL/min. The detection wavelength was 262 nm.

The intermediates were analyzed using LC-TOF-MS (Agilent 6210) in negative electrospray ionization mode (ESI<sup>-</sup>)<sup>3, 4</sup>. Separation was performed using an a C18 column (Agilent eclipse XDB-C18, 4.6 mm × 300 mm, 5 μm). The mobile phase consisted of methanol (A) and water (B) with a gradient elution of A/B (v/v) from 25/75 to 100/0 linearly in 25 min at a flow rate of 1 mL/min during the detection. All data collected were acquired and processed using Agilent Mass Hunter Qualitative Analysis.

#### **Text S5 Methods for Fourier transform ion cyclotron resonance mass spectrometer (FT-ICR-MS) and data analysis**

Solid phase extraction (SPE)

Oasis HLB SPE cartridges were conditioned with 12 mL methanol and 12 mL 0.01 mol/L HCl sequentially before sample loading. Approximately 100 mL sample, of which pH were pre-adjusted to < 2 by formic acid, was loaded. After that, cartridges were rinsed with 18 mL 0.01 mol/L HCl and eluted with 12 mL methanol. The methanol was collected and concentrated to 1 mL with  $\text{N}_2$ .

FT-ICR-MS analysis

The prepared samples were analyzed by a 7.0 T Fourier transform ion cyclotron resonance mass spectrometer (FT-ICR-MS)(SolariX, Bruker) equipped with an electrospray ionization (ESI) source in negative mode<sup>5, 6</sup>. Peaks identified in mass spectra from 100 to 1500 m/z. Molecular formulas of products were calculated using Data Analysis software. Elemental combinations were limited to molecular formulas containing  $^{12}\text{C}_{0-100}$ ,  $^1\text{H}_{0-200}$ ,  $^{14}\text{N}_{0-4}$ ,  $^{16}\text{O}_{0-30}$ , and mass peaks with Signal-to-Noise Ratio greater than 6 were considered during molecule assignment. The errors between measured

MW and the theoretical one was set to < 1.

DBE values were determined by Eq.S4<sup>7</sup>

$$DBE=C-\frac{1}{2}H+\frac{1}{2}N+1 \quad (S4)$$

where C, O, H and N represent the number of atoms in a given formula.

AI values were calculated by Eq.s5<sup>8</sup>(S/P/Cl was not in consideration)

$$AI=[1+C-O-\frac{1}{2}H]/[C-N-O] \quad (S5)$$

Note, if  $[1+C-O-\frac{1}{2}H]<0$  or  $[C-N-O]<0$ , then AI was defined as 0.

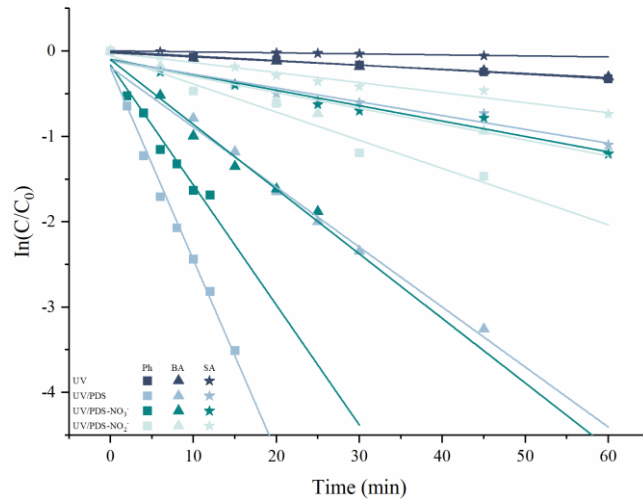


**Fig.S1 kinetic of pollutants' removal**  
 ( $[\text{NO}_3^-]=[\text{NO}_2^-]=2 \text{ mM}$ ,  $[\text{pollutant}]=0.1 \text{ mM}$ )

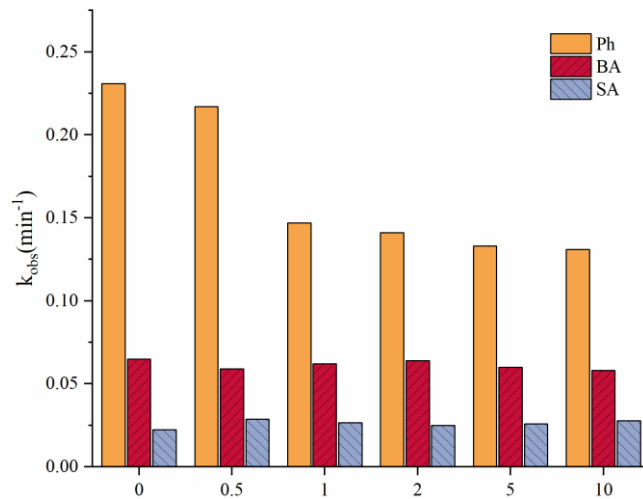


**Fig.S2 kinetic of pollutants' removal in UV/PDS with different addition of  $\text{NO}_3^-$**   
 ( $[\text{pollutant}]=0.1 \text{ mM}$ )

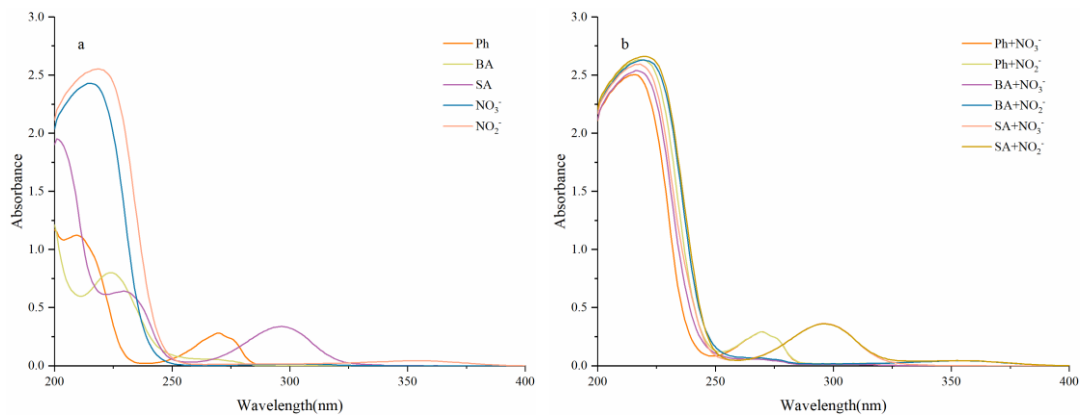


**Fig.S3 Absorbance of  $\text{NO}_3^-$ ,  $\text{NO}_2^-$  and the three compounds(a), Absorbance of three compounds with the addition of  $\text{NO}_3^-/\text{NO}_2^-$ (b)**  
 ( $[\text{NO}_3^-]=[\text{NO}_2^-]=2 \text{ mM}$ ,  $[\text{pollutant}]=0.1 \text{ mM}$ )

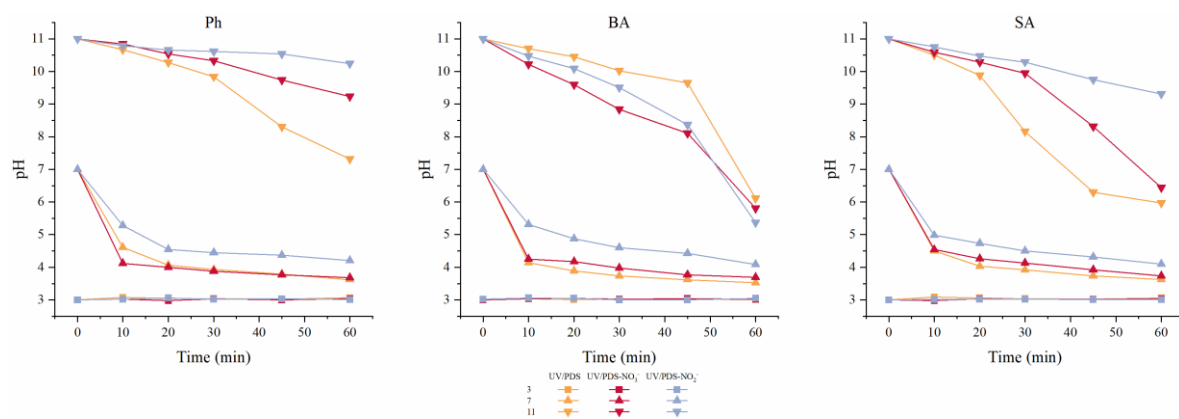


**Fig. S4 pH variation during the reaction**

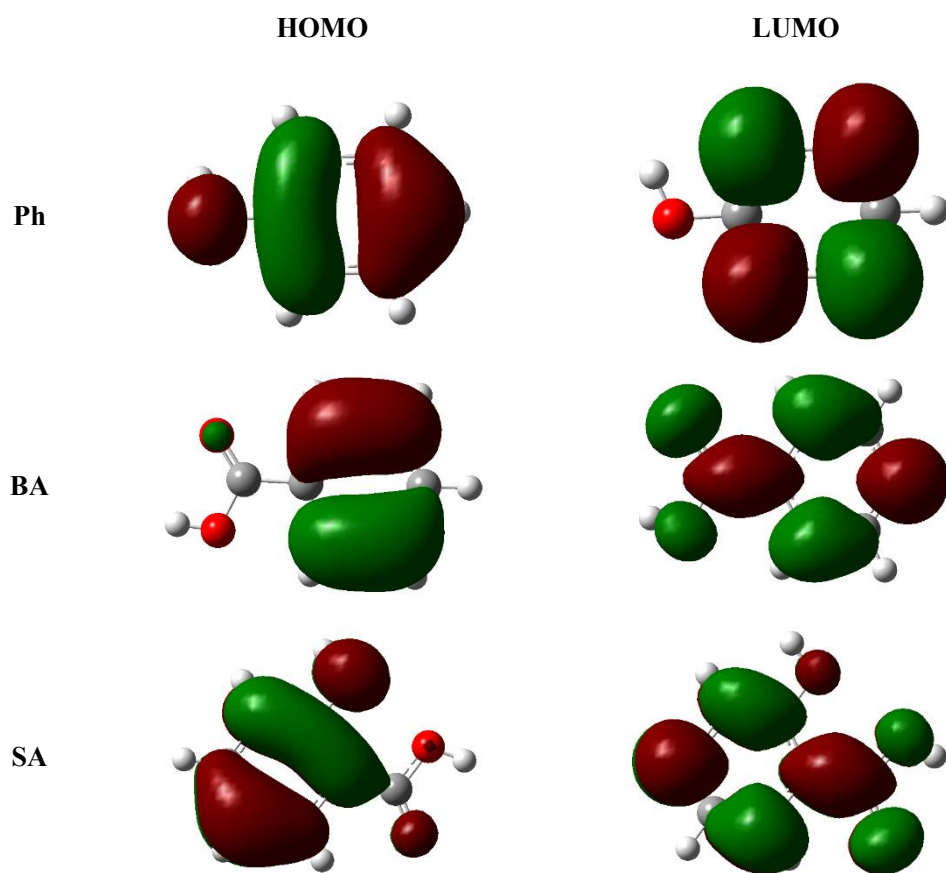


**Fig. S5 The HOMO and LUMO distribution of Ph, BA and SA calculated at B3LYP/6-31+G(d) level.**

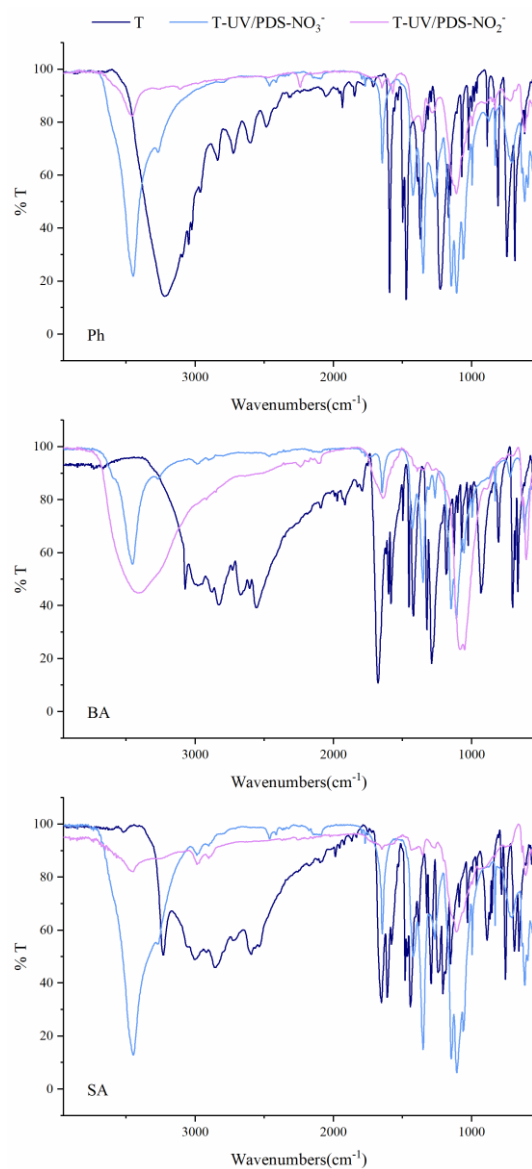


**Fig. S6 FT IR spectra of three compounds before and after treatment with species**

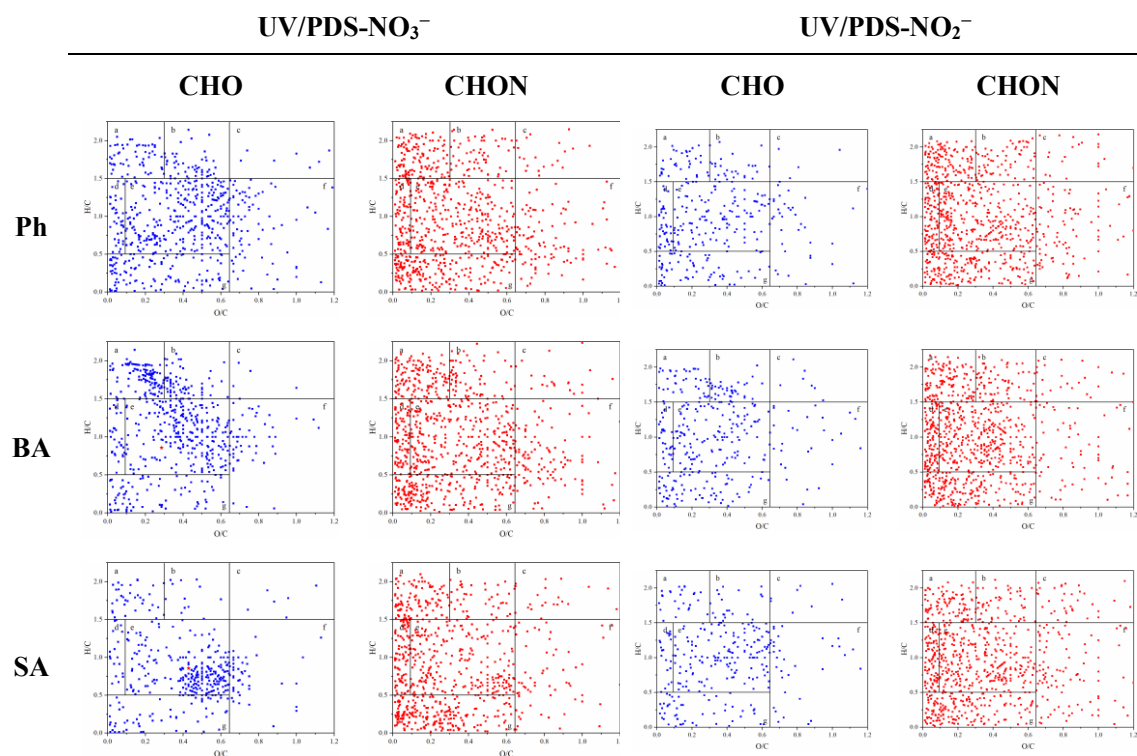


**Fig. S7** Van Krevelen diagrams of potentially formed CHO (blue) and CHON (red) of Ph, BA and SA during UV/PDS oxidation in the presence of NO<sub>3</sub><sup>-</sup> and NO<sub>2</sub><sup>-</sup>

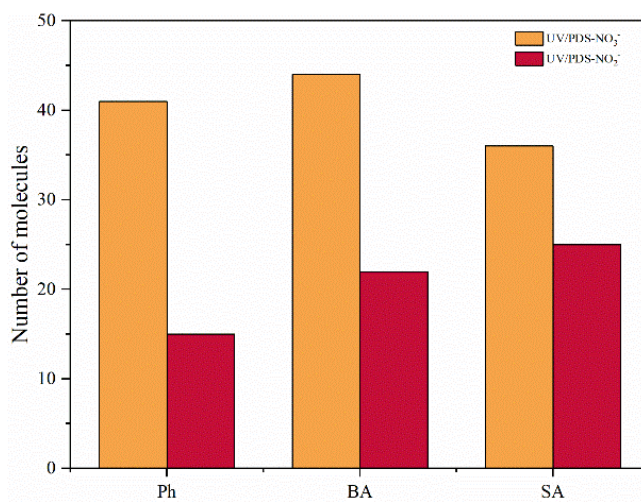


**Fig. S8** Molecule number of byproducts of Ph, BA and SA treated by UV/PDS in the presence of NO<sub>3</sub><sup>-</sup> and NO<sub>2</sub><sup>-</sup>

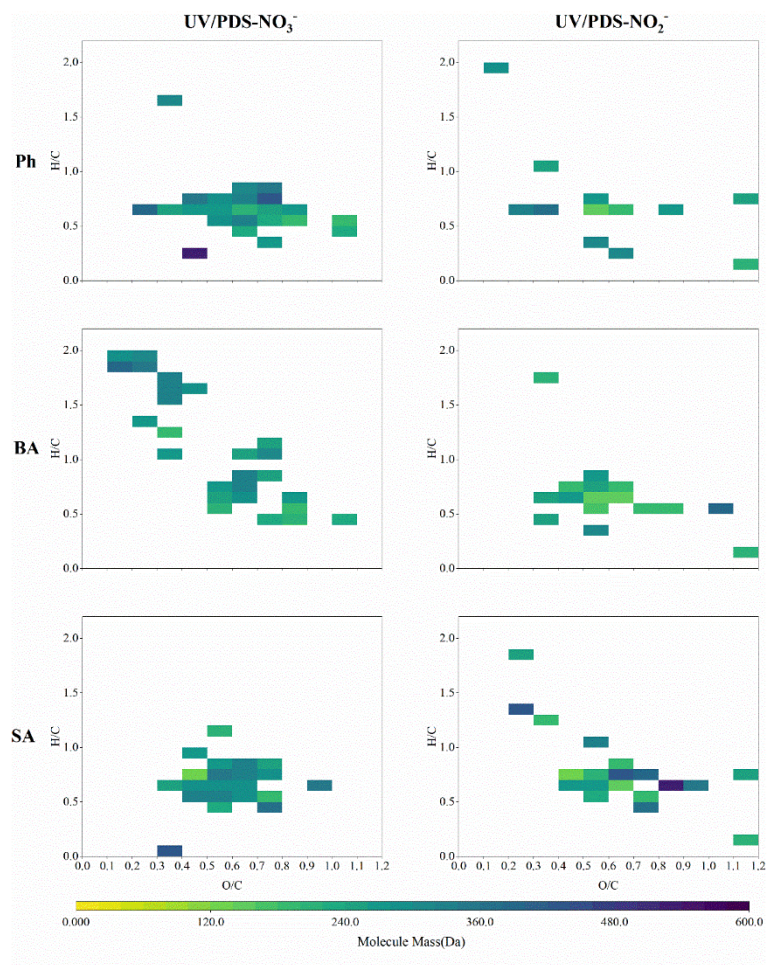


**Fig. S9** Distribution of molecule mass of byproducts of Ph, BA and SA in UV/PDS in the presence of NO<sub>3</sub><sup>-</sup> and NO<sub>2</sub><sup>-</sup>

**Table S1 Comparison of the reaction stoichiometric efficiency in different systems**

Compounds		%RSE	References
Ph	UV/PDS	84.4	This study
	UV/PDS-NO <sub>3</sub> <sup>-</sup>	73.5	
	UV/PDS-NO <sub>2</sub> <sup>-</sup>	27.5	
BA	UV/PDS	44.7	This study
	UV/PDS-NO <sub>3</sub> <sup>-</sup>	30.8	
	UV/PDS-NO <sub>2</sub> <sup>-</sup>	23.4	
SA	UV/PDS	27.7	This study
	UV/PDS-NO <sub>3</sub> <sup>-</sup>	16.4	
	UV/PDS-NO <sub>2</sub> <sup>-</sup>	15.8	
chloramphenicol	UV/PS [PS]=0.25 mM	45	9
	UV/PS [PS]=0.5 mM	24	
Sulfamethoxazole	AgFe/PS	10	10
	CoFe/PS	9	
	Fe/PS	6	
bisoprolol	Heat/PS	82	11

**Table S2 Calculated condensed Fukui function and dual descriptor of Ph**

Atom	Num	q (N)	q (N+1)	q (N-1)	$f^-$	$f^+$	$f^0$
C	1	-0.2383	-0.4416	-0.2071	0.0312	0.2033	0.1172
C	2	-0.3186	-0.5144	-0.2195	0.0991	0.1958	0.1474
C	3	0.2969	0.3045	0.4338	0.1369	-0.0076	0.0646
C	4	-0.3059	-0.5095	-0.1974	0.1085	0.2036	0.1561
C	5	-0.2393	-0.4341	-0.2177	0.0216	0.1949	0.1082
C	6	-0.2891	-0.2916	-0.0490	0.2401	0.0025	0.1213
H	7	0.2601	0.2226	0.2913	0.0312	0.0375	0.0343
H	8	0.2629	0.2268	0.2964	0.0335	0.0361	0.0348
H	9	0.2635	0.2269	0.2972	0.0337	0.0367	0.0352
H	10	0.2598	0.2227	0.2907	0.0309	0.0371	0.0340
H	11	0.2582	0.2310	0.2878	0.0297	0.0272	0.0284
O	12	-0.7548	-0.7783	-0.5793	0.1755	0.0235	0.0995
H	13	0.5445	0.5348	0.5728	0.0282	0.0097	0.0190

**Table S3** Calculated condensed Fukui function and dual descriptor of BA

Atom	Num	q (N)	q (N+1)	q (N-1)	$f^-$	$f^+$	$f^0$
C	1	-0.1983	-0.2966	-0.1326	0.0657	0.0984	0.0820
C	2	-0.2535	-0.2759	-0.2171	0.0365	0.0224	0.0294
C	3	-0.2147	-0.3789	0.0477	0.2624	0.1642	0.2133
C	4	-0.2536	-0.2743	-0.1512	0.1025	0.0207	0.0616
C	5	-0.1940	-0.2963	-0.1873	0.0067	0.1023	0.0545
C	6	-0.1905	-0.2606	0.0792	0.2696	0.0701	0.1699
H	7	0.2723	0.2457	0.3037	0.0314	0.0266	0.0290
H	8	0.2658	0.2428	0.2978	0.0320	0.0230	0.0275
H	9	0.2650	0.2363	0.2935	0.0285	0.0287	0.0286
H	10	0.2659	0.2430	0.2976	0.0317	0.0229	0.0273
H	11	0.2708	0.2440	0.3028	0.0320	0.0268	0.0294
C	12	0.8272	0.6688	0.7949	-0.0324	0.1584	0.0630
O	13	-0.6858	-0.8401	-0.5936	0.0922	0.1543	0.1232
O	14	-0.7320	-0.7924	-0.7048	0.0272	0.0604	0.0438
H	15	0.5553	0.5345	0.5695	0.0142	0.0209	0.0175

**Table S4** Calculated condensed Fukui function and dual descriptor of SA

Atom	Num	q (N)	q (N+1)	q (N-1)	$f^-$	$f^+$	$f^0$
C	1	-0.3143	-0.3634	-0.1793	0.1350	0.0490	0.0920
C	2	0.3596	0.2991	0.4722	0.1126	0.0604	0.0865
C	3	-0.2427	-0.3044	-0.1666	0.0761	0.0617	0.0689
C	4	-0.1784	-0.3068	-0.1179	0.0604	0.1284	0.0944
C	5	-0.2838	-0.2910	-0.0499	0.2338	0.0072	0.1205
C	6	-0.1966	-0.3606	-0.2006	-0.0039	0.1640	0.0800
H	7	0.2691	0.2438	0.3018	0.0327	0.0252	0.0289
H	8	0.2720	0.2443	0.3024	0.0304	0.0276	0.0290
H	9	0.2656	0.2427	0.2952	0.0295	0.0228	0.0262
H	10	0.2672	0.2370	0.2972	0.0299	0.0302	0.0301
C	11	0.8246	0.6715	0.8216	-0.003	0.1530	0.0750
O	12	-0.6973	-0.8444	-0.6511	0.0463	0.1471	0.0967
O	13	-0.7223	-0.7803	-0.7082	0.0140	0.0579	0.0360
H	14	0.5508	0.5294	0.5610	0.0101	0.0214	0.0157
O	15	-0.7215	-0.7530	-0.5536	0.1679	0.0314	0.0997
H	16	0.5479	0.5358	0.5757	0.0277	0.0121	0.0199

## References

1. X. Ao, X. Zhang, W. Sun, K. G. Linden, E. M. Payne, T. Mao and Z. Li, *Water Research*, 2024, **253**.
2. Y. Huang, M. Kong, D. Westerman, E. G. Xu, S. Coffin, K. H. Cochran, Y. Liu, S. D. Richardson, D. Schlenk and D. D. Dionysiou, *Environmental Science & Technology*, 2018, **52**, 12697-12707.
3. M. J. Martínez Bueno, A. Agüera, M. J. Gómez, M. D. Hernando, J. F. García-Reyes and A. R. Fernández-Alba, *Analytical Chemistry*, 2007, **79**, 9372-9384.
4. X. Gao, Q. Zhang, Z. Yang, Y. Ji, J. Chen and J. Lu, *ACS ES&T Engineering*, 2022, **2**, 222-231.
5. H. Xu, Y. Li, M. Ding, W. Chen, K. Wang and C. Lu, *Water Research*, 2018, **143**, 250-259.
6. L. Xiao, S. Hu, H. Han, Q. Ren, L. He, L. Jiang, S. Su, Y. Wang and J. Xiang, *Journal of Analytical and Applied Pyrolysis*, 2021, **156**.
7. L. R. Mazzoleni, P. Saranjampour, M. M. Dalbec, V. Samburova, A. G. Hallar, B. Zielinska, D. H. Lowenthal and S. Kohl, *Environmental Chemistry*, 2012, **9**.
8. B. P. Koch and T. Dittmar, *Rapid Communications in Mass Spectrometry*, 2006, **20**, 926-932.
9. A. Ghauch, A. Baalbaki, M. Amasha, R. El Asmar and O. Tantawi, *Chemical Engineering Journal*, 2017, **317**, 1012-1025.
10. G. Ayoub and A. Ghauch, *Chemical Engineering Journal*, 2014, **256**, 280-292.
11. A. Ghauch and A. M. Tuqan, *Chemical Engineering Journal*, 2012, **183**, 162-171.